

Differential α -adrenergic modulation of rapid onset vasodilatation along resistance networks of skeletal muscle in old *versus* young mice

Shenghua Y. Sinkler¹, Charmain A. Fernando¹ and Steven S. Segal^{1,2}

¹Department of Medical Pharmacology and Physiology, University of Missouri, Columbia, MO 65212, USA

²Dalton Cardiovascular Research Center, Columbia, MO 65211, USA

Key points

- Rapid onset vasodilatation (ROV) initiates functional hyperaemia upon skeletal muscle contraction and is attenuated during ageing via α -adrenoreceptor (α AR) stimulation, but it is unknown where this effect predominates in resistance networks.
- In gluteus maximus muscles of young (4 months) and old (24 months) male C57BL/6 mice, tetanic contraction while observing feed arteries and arterioles initiated ROV, which increased with contraction duration, peaked later in upstream *versus* downstream vessel branches and was attenuated throughout networks with advanced age.
- With no effect on muscle force production, inhibiting α ARs improved ROV in old mice while activating α ARs attenuated ROV in young mice.
- Modulating ROV through α ARs was greater in upstream feed arteries and arterioles compared to downstream arterioles, with α_2 ARs more effective than α_1 ARs.
- ROV is coordinated along resistance networks and modulated differentially between young and old mice via α ARs; with advanced age, attenuated dilatation of upstream branches will restrict muscle blood flow.

Abstract Rapid onset vasodilatation (ROV) in skeletal muscle is attenuated during advanced age via α -adrenoreceptor (α AR) activation, but it is unknown where such effects predominate in the resistance vasculature. Studying the gluteus maximus muscle (GM) of anaesthetized young (4 months) and old (24 months) male C57BL/6 mice, we tested the hypothesis that attenuation of ROV during advanced age is most effective in proximal branches of microvascular resistance networks. Diameters of a feed artery (FA) and first- (1A), second- (2A) and third- (3A) order arterioles were studied in response to single tetanic contractions (100 Hz, 100–1000 ms). ROV began within 1 s and peaked sooner in 2A and 3A (~ 3 s) than in 1A or FA (~ 4 s). Relative amplitudes of dilatation increased with contraction duration and with vessel branch order (FA < 1A < 2A < 3A). In old mice, attenuation of ROV was greater in FA and 1A compared to 2A and 3A. With no effect on muscle force production, inhibiting α ARs (phentolamine; 10^{-6} M) improved ROV in FA and 1A of old mice while subthreshold stimulation of α ARs in young mice (noradrenaline; 10^{-9} M) depressed ROV most effectively in FA and 1A. In young mice, stimulating α_1 ARs (phenylephrine; 10^{-7} M) and α_2 ARs (UK 14304; 10^{-7} M) attenuated ROV primarily in FA. In old mice, inhibiting α_2 ARs (rauwolscine; 10^{-7} M) restored ROV more effectively in FA and 1A than did inhibiting α_1 ARs (prazosin; 10^{-8} M). We conclude that, with temporal and spatial coordination along resistance networks, attenuation of ROV with advanced age is most effective in proximal branches via constitutive activation of α_2 ARs.

(Received 9 March 2016; accepted after revision 27 July 2016; first published online 8 August 2016)

Corresponding author S. S. Segal: Department of Medical Pharmacology and Physiology, 1 Hospital Drive, MA415 Medical Science Building, University of Missouri, Columbia, MO 65212, USA. Email: segalss@health.missouri.edu

Abbreviations 1A, first-order arteriole; 2A, second-order arteriole; 3A, third-order arteriole; α AR, α -adrenoreceptor; FA, feed artery; fps, frames per second; GM, gluteus maximus muscle; ID, internal diameter; NA, noradrenaline; PE, phenylephrine; PGP, protein gene product; PZ, prazosin; ROI, region of interest; ROV, rapid onset vasodilatation; RW, rauwolscine; Phentol, phentolamine; PSS, physiological salt solution; TH, tyrosine hydroxylase; SMC, smooth muscle cell; SNA, sympathetic nerve activity; SNP, sodium nitroprusside; UK, UK 14304.

Introduction

Rapid onset vasodilatation (ROV) reflects the near-instantaneous relaxation of smooth muscle cells (SMCs) of the resistance vasculature in response to skeletal muscle contraction (Corcondilas *et al.* 1964; Tschakovsky *et al.* 1996; Mihok & Murrant, 2004; VanTeeffelen & Segal, 2006). Through initiating the increase in blood flow to active muscle fibres, ROV facilitates the transition from rest to physical activity. These same vessels are surrounded by sympathetic nerves which release noradrenaline (NA) to evoke vasoconstriction that increases with the level of α -adrenoreceptor (α AR) activation (Marshall, 1982; Faber, 1988). As shown with microneurography in human subjects, sympathetic nerve activity (SNA) increases with exercise intensity and active muscle mass (Seals, 1989*a,b*). The autonomic nervous system remains active under resting conditions and the background level of SNA increases with advanced age in humans (Dinenno *et al.* 1999; Fisher & Paton, 2012). Enhanced SNA during advanced age is also implicated in rodents. For example, release of NA from sympathetic nerves into the circulation was greater at rest and during immobilization stress in aged (24 months) compared to young adult (3 months) male Fischer-344 rats (McCarty *et al.* 1997). Further, tyrosine hydroxylase activity, which governs NA synthesis, was \sim 2-fold higher in adrenal glands of old (24 months) compared to young (4 months) male rats and mice (Reis *et al.* 1977). Such similarities between species support the use of rodents as models that enable more invasive studies of how advanced age affects the role of sympathetic neuro-effector signalling in modulating muscle blood flow.

Functional sympatholysis describes the inhibition of sympathetic vasoconstriction during muscular activity (Remensnyder *et al.* 1962) and is impaired in humans with advanced age (Dinenno *et al.* 2005). Further, the ability to rapidly increase muscle blood flow in response to muscle contraction is attenuated in older (>60 years) compared to younger (\sim 20–30 years) humans (Carlson *et al.* 2008; Casey & Joyner, 2012). Attenuated muscle blood flow with diminished vascular conductance can reflect the activation of α ARs (Dinenno *et al.* 1999; Casey & Joyner, 2012). Thus, blocking α ARs with phentolamine restored ROV to forearm muscle contractions in old adults (\sim 69 years), whereas increasing SNA (via lower body negative pressure) impaired ROV in younger subjects (\sim 27 years) (Casey & Joyner, 2012). The effect of enhanced α AR activation during advanced age on ROV is also manifest in the

mouse. Thus, attenuated ROV of distributing (i.e. second order) arterioles in the gluteus maximus muscle (GM) of old (20 months) male mice was restored to that of young (3–4 months) male mice by topical superfusion of phentolamine (Jackson *et al.* 2010). However, these initial studies did not address other branches of the resistance network and the regulation of blood flow requires coordinated activity among upstream and downstream branches (Segal & Duling, 1986; Segal, 2005). In such manner, volume flow into the muscle is governed by proximal feed arteries (FAs) and first-order (1A) arterioles, with regional distribution governed by second- (2A) and third-order (3A) arterioles downstream; the latter give rise to terminal arterioles and capillaries. Whilst sympathetic vasoconstriction reflects the activation of α ARs on SMCs, the functional distribution of α_1 AR and α_2 AR subtypes vary with microvessel branch order (Boegehold & Johnson, 1988; Faber, 1988; Dodd & Johnson, 1993; Moore *et al.* 2010*b*). With advanced age (24 *versus* 4 months) in the mouse GM, response curves to progressive α_1 AR activation were maintained in FA and 1A branches while attenuated in 2A and 3A branches, while during α_2 AR activation the efficacy of constriction decreased as vessel branch order increased (Sinkler & Segal, 2014). Such regional differences in adrenergic reactivity suggest that modulation of ROV by α_1 AR *versus* α_2 AR activation may vary among upstream and downstream branches. However, it is unknown how the activation or inhibition of α ARs may affect ROV in respective branch orders, nor how these relationships are affected by advanced age.

A limitation when studying blood flow responses to contractile activity in skeletal muscle of human subjects is the inability to resolve the dynamics of the actual site(s) of vascular resistance. To elucidate such behaviour requires invasive methods, for which the mouse GM is well-suited (Bearden *et al.* 2004; Jackson *et al.* 2010; Moore *et al.* 2010*a*; Sinkler & Segal, 2014; Fernando *et al.* 2016). The GM is a powerful hip extensor of mixed fibre type (Lampa *et al.* 2004; Manttari & Jarvilehto, 2005) which is typical of human skeletal muscle (Saltin *et al.* 1977; Lexell, 1995). Using the mouse GM, the goal of this study was to evaluate ROV in proximal FA and 1A as well as distal 2A and 3A branches of intact microvascular resistance networks controlling blood flow to skeletal muscle fibres *in vivo*. Diameter responses of respective branch orders to graded single tetanic contractions were recorded in young and old mice before and during selective stimulation or inhibition of α_1 ARs and α_2 ARs. We tested the hypothesis that ROV

is attenuated most effectively in proximal branches of the resistance network during advanced age.

Methods

Animal care and use

Experimental protocols were approved by the Animal Care and Use Committee of the University of Missouri and were performed in accordance with the National Research Council's *Guide for the Care and Use of Laboratory Animals* (2011). For ROV experiments, young (4 months; $n = 12$, 30.9 ± 0.5 g) and old (24 months; $n = 12$, 32.3 ± 0.7 g) C57BL/6 male mice were obtained from National Institute on Aging colonies (Charles River Laboratories, Wilmington, MA, USA). Respective age groups in mice correspond to humans in their middle 20s and late 60s (Flurkey *et al.* 2007). All mice were acclimated in animal care facilities of the University of Missouri for at least one week before being studied. Room temperature was maintained at $\sim 24^\circ\text{C}$ on a 12h:12h (light:dark) cycle with food and water available *ad libitum*. One mouse was studied each day alternating between young and old mice. On the morning of an experiment, a mouse was anaesthetized by intraperitoneal injection of pentobarbital sodium (60 mg kg^{-1}) and supplemented as needed (20 mg kg^{-1}) to maintain anaesthesia. Esophageal temperature was maintained at $\sim 37^\circ\text{C}$ by placing the mouse on an aluminum warming plate ($5 \text{ cm} \times 11 \text{ cm}$). Upon completion of the experimental protocol (duration, $\sim 5\text{--}6$ h), the mouse was killed by an overdose of pentobarbital sodium (intraperitoneal injection) followed by cervical dislocation.

Gluteus maximus muscle preparation

The GM was prepared by shaving the left hindquarter then placing the mouse in the prone position on the warming plate. The skin and connective tissue overlying the left GM was removed and exposed tissue was superfused continuously at 3 ml min^{-1} with bicarbonate buffered physiological salt solution (PSS) that contained (in mM): 131.9 NaCl, 4.7 KCl, 2 CaCl₂, 1.17 MgSO₄, 18 NaHCO₃ and equilibrated with 5% CO₂–95% N₂ ($34\text{--}35^\circ\text{C}$, pH 7.4). While viewing through a stereomicroscope, the left GM was carefully dissected along its origin, reflected away from the hindquarter onto a transparent rubber pedestal (Sylgard 184; Dow Corning, Midland, MI, USA) and the edges pinned to approximate its dimensions *in situ*. Superficial connective tissue and fat were carefully removed to expose the resistance network including the FA (i.e. the inferior gluteal artery), which becomes the 1A upon entering the muscle, and the downstream 2A and 3A branches. The inferior gluteal motor nerve bundle was cut proximally and the free end aspirated into an insulated

borosilicate glass microelectrode filled with PSS (Moore *et al.* 2010a). To minimize stray current, the interface between the nerve and suction electrode was insulated with Kwik-Cast Sealant (World Precision Instruments, Inc. USA). The completed preparation was transferred to the fixed stage of an intravital microscope (Nikon E600FN; Melville, NY, USA) mounted on an X–Y translational stage (Gibraltar; Burleigh Instruments, Fishers, NY, USA).

Intravital microscopy

Images were acquired through a Nikon SLWD $\times 20$ objective (numerical aperture = 0.35) focused onto a FireWire colour charge-coupled device camera (DFK 21AF04; The Imaging Source, Charlotte, NC, USA). Spatial resolution on the video monitor was $\sim 1 \mu\text{m}$. Digital images were recorded at 30 frames per second (fps) on a personal computer using custom LabView software (National Instruments, Austin, TX, USA) provided by Dr Michael J. Davis (University of Missouri, Columbia, MO, USA). The internal diameter (ID; defined as the widest distance between edges of the lumen) of each vessel studied was measured frame-by-frame during playback using a video caliper integrated into the software. Each GM preparation was equilibrated for 30 min before evaluating initial resting diameters prior to GM contractions (Fig. 1). Data were acquired only from preparations exhibiting robust vasomotor tone under resting conditions (Sinkler & Segal, 2014). At the end of each experiment, maximal diameters were recorded during superfusion with sodium nitroprusside (SNP, 10^{-4} M).

Muscle stimulation to evoke ROV

Single tetanic contractions of the inferior GM were induced by electrical stimulation of the motor nerve (30 V, 100 Hz, 0.1 ms pulse) for durations of 100, 250, 500 and 1000 ms. Stimulation at 100 Hz evokes maximal tetanic force production (Bearden *et al.* 2004; Fernando *et al.* 2016) and this range of contraction durations encompasses the initiation of ROV in all branch orders (100 ms) through attaining near-maximal dilatation in distal (2A and 3A) branches (1000 ms). Stimuli were delivered through a SIU5 stimulus isolation unit driven by a square wave stimulator (S48; Grass Instruments, Quincy, MA, USA). In preliminary studies, visual observation through the stereomicroscope confirmed that arterioles and venules within the GM were compressed during contraction; concomitant monitoring of output from the stimulator verified that the onset and cessation of electrical stimulation coincided with the onset and cessation of muscle contraction. One vessel (FA, 1A, 2A, or 3A) was observed for each set of four contractions, with the order of respective branches randomized across experiments. Each vessel recovered to its resting baseline

diameter within several minutes following a contraction. In this manner, evaluating ROV to four contraction durations in four branch orders during a given condition required 16 separate contractions, with three series of contractions (control + 2 experimental treatments) performed in each GM preparation. Preliminary control experiments confirmed that vasomotor tone and ROV remained stable throughout four series of contractions performed in this manner.

Analysis of ROV. Diameter responses of FA, 1A, 2A, and 3A branches during ROV were obtained from frame by frame measurements of ID during offline analyses of video recordings. 'Peak' vasodilatation refers to the largest ID recorded in response to a contraction and is

used to express the amplitude of ROV. The calculated diameter change = $ID_{\text{peak}} - ID_{\text{rest}}$, where ID_{rest} = baseline ID preceding each contraction. To facilitate comparison of responses across vessel branch orders, vasodilatation is expressed as a percentage of respective maximal IDs during superfusion with 10^{-4} M SNP and calculated as: $\text{vasodilatation (\% max)} = [(ID_{\text{response}} - ID_{\text{rest}})/(ID_{\text{max}} - ID_{\text{rest}})] \times 100\%$, where ID_{response} = ID at designated time point(s) following contraction and ID_{max} = maximal ID during SNP. Temporal aspects of ROV were defined with respect to the cessation of contraction, which was taken as the '0' time point for ROV. Due to tissue displacement during contraction, the 'onset' of ROV was evaluated at 1 s post contraction as this was the earliest time point that images were refocused consistently. The time-to-peak ROV was defined as the interval between the end of contraction and attaining the peak response ID.

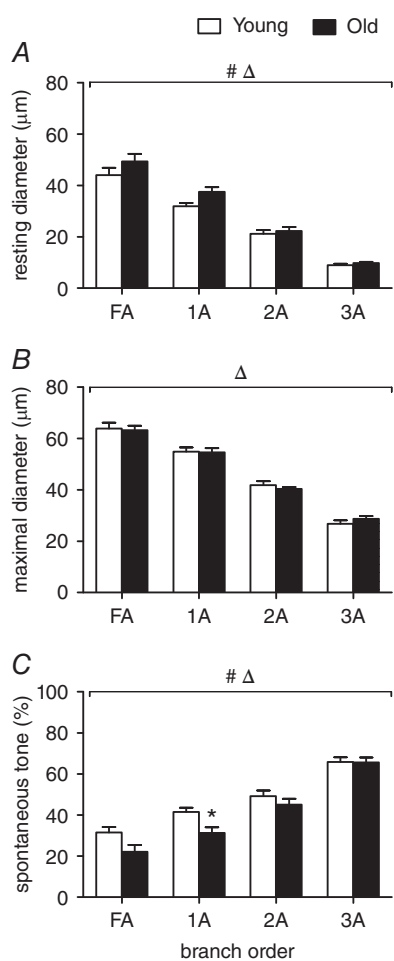


Figure 1. Internal diameters and spontaneous tone in GM feed arteries and arterioles are similar for young and old mice

Resting diameter (A) and maximal diameter (B) decreased as vessel branch order increased for both age groups (FA > 1A > 2A > 3A). Spontaneous tone (C; see Methods) increased with vessel branch order. Summary data are means ± SEM, $n = 6$ per age group. # $P < 0.05$, main effect of age. Δ $P < 0.05$, main effect of vessel branch order; * $P < 0.05$, old vs. young mice for designated branch order.

Pharmacology

Pharmacological treatments were added to the superfusion solution for topical application at a designated concentration (Sinkler & Segal, 2014). The GM preparation was equilibrated with respective treatments for 20 min before measurements were performed while the treatment was maintained. Non-selective stimulation of α ARs used 10^{-9} M NA and non-selective inhibition of α ARs used 10^{-6} M phentolamine (Jackson *et al.* 2010; Moore *et al.* 2010b). The effects of selective inhibition of α_1 ARs or α_2 ARs on ROV were investigated using 10^{-8} M prazosin (PZ) or 10^{-7} M rauwolscine (RW), respectively (Moore *et al.* 2010b). The effects of selective stimulation of α_1 ARs and α_2 ARs on ROV was investigated using 10^{-6} M phenylephrine (PE) and 10^{-6} M UK 14304 (UK), respectively (Moore *et al.* 2010b). The order of respective treatments varied across experiments. All compounds for pharmacological interventions were dissolved in PSS except for UK 14304, which was first dissolved in DMSO (final concentration, 0.0001%). Reagents were obtained from Sigma Chemical Co. (St Louis, MO, USA) unless indicated otherwise.

Muscle force production

Eight additional mice ($n = 6$ young + 2 old; as above) were studied to determine whether GM contractile function was affected during either stimulation or inhibition of α ARs. The force produced during each tetanic contraction was measured as described (Bearden *et al.* 2004; Fernando *et al.* 2016) under control conditions, in the presence of 10^{-9} M NA and (following a 30 min wash) in the presence of phentolamine (10^{-6} M). For these experiments, the GM was dissected along its origin and reflected away from the hindquarter (as above) then secured in an

atraumatic clamped positioned across its midline (i.e. perpendicular to muscle fibres). The clamp was attached to a calibrated load beam (LCL-1136; Omega, Stamford, CT, USA; resolution ± 0.1 g) mounted on a micrometer spindle that enabled muscle length to be adjusted for optimal force production (L_0). Output from the load beam was amplified (TBM-4; World Precision Instruments, Sarasota, FL, USA) and recorded at 2 kHz (PowerLab/4SP; ADInstruments Inc; Colorado Springs, CO, USA) with a personal computer. Using electrical field stimulation (20 V, 100 Hz, 0.1 ms pulse) between platinum–iridium (90%–10%) wire electrodes (diameter, 250 μ m), tetanic contractions were evoked for 100, 250 500 and 1000 ms (as done for ROV). The muscle was then cut free from both its insertion and the muscle clamp, blotted of excess moisture and its wet weight (W_w) measured (± 0.01 mg) on a microbalance (XS105, Mettler Toledo; Columbia, OH, USA). Muscle cross-section area (mm^2) was calculated as:

$$[W_w \text{ (mg)} / \{(L_0 \text{ (mm)} \times \text{muscle density (1.06 mg/mm}^3)\})].$$

After subtracting resting tension, active force was expressed as millinewtons per mm^2 (mN/mm^2).

Immunofluorescence

To confirm the presence of perivascular sympathetic innervation, individual FAs were dissected and pinned in a Petri dish coated with Sylgard, fixed in 4% paraformaldehyde for 20 min, blocked with 10% normal goat serum and incubated overnight at 4°C with primary antibodies for tyrosine hydroxylase (TH; dilution, 1:250; No. T2928, Sigma) to identify sympathetic nerves (Loofth-Wilson *et al.* 2004) and for protein gene product 9.5 (PGP 9.5; dilution, 1:400; UltraClone Ltd, Isle of Wight, UK) to identify all perivascular nerves (Thompson *et al.* 1983). Vessels were incubated with secondary antibodies (1:500 dilution) for 90 min at room temperature (Alexa Fluor-488 or -546; Molecular Probes/Life Technologies; Carlsbad, CA; USA) then transferred to a glass slide and mounted with ProLong Gold (Invitrogen). Cover slips were applied and sealed with clear nail polish. Between each incubation step, vessels were rinsed 3 times in phosphate-buffered saline (PBS; No. P5368, Sigma). Primary and secondary antibodies were diluted in PBS + 0.2% Triton X-100. Labelled vessel segments were imaged on a Leica SP5 confocal microscope using a HCX PL APO $\times 40$ oil immersion objective (numerical aperture, 1.25) with a $\times 2$ optical zoom and 1 μ m Z-slices.

Innervation density was evaluated by quantifying the fluorescence area of TH and PGP9.5 staining on FA segments using Image J as described (Boerman & Segal, 2016). Briefly, a maximum Z-stack projection was created through the upper half of the vessel wall by taking the

Table 1. Resting diameters are maintained during stimulation and inhibition of α ARs

	Young			Old		
	Control	NA	Phentol	Control	NA	Phentol
FA	38 \pm 2	38 \pm 1	36 \pm 3	43 \pm 3	43 \pm 3	42 \pm 3
1A	30 \pm 2	29 \pm 1	29 \pm 1	34 \pm 2	34 \pm 2	33 \pm 2
2A	20 \pm 1	20 \pm 1	19 \pm 1	21 \pm 1	21 \pm 1	20 \pm 1
3A	10 \pm 1	10 \pm 1	9 \pm 1	9 \pm 1	9 \pm 1	9 \pm 1

Compared to control, subthreshold stimulation with noradrenaline (NA, 10^{-9} M) or phentolamine (Phentol, 10^{-6} M) had no significant effect on internal diameters (μ m) of any vessel branch order in the GM of either young or old mice. Summary data are means \pm SEM, $n = 6$ per age group.

maximum intensity value of each pixel through the series of confocal slices and combining these pixel values into a single image. A region of interest (ROI) was placed around the entire projection, background fluorescence was subtracted and the remaining fluorescent pixels were quantified relative to the total number of pixels in the ROI to yield the percentage fluorescence area within the ROI for each antibody. Controls confirmed lack of imaging bleed-through between respective secondary antibodies.

Statistics

Data were analysed with two-way analysis of variance (ANOVA) and linear regression to evaluate the effect of vessel branch order and age on ROV. Two-way repeated measures ANOVA was used to evaluate main effects of pharmacological interventions with respect to vessel branch order and GM force production. *Post hoc* comparisons were performed using Bonferroni tests. Summary data are expressed as means \pm SEM. Differences were considered statistically significant with $P < 0.05$.

Results

Resting and maximal diameters are similar for GM of young and old mice

Internal diameters were similar between young and old mice across all branch orders at rest and during maximal dilatation with 10^{-4} M SNP (Fig. 1). Spontaneous vasomotor tone at rest was similar between age groups but slightly larger resting diameters for 1A in the GM of old mice was reflected in significantly lower spontaneous tone in this branch order (Fig. 1C). Subthreshold activation of α ARs with 1 nM NA had no effect on resting diameters, nor did inhibition of α ARs with 1 μ M phentolamine (Table 1).

ROV is blunted during advanced age throughout resistance networks

Single tetanic contractions evoked ROV in all vessel branch orders of both young and old mice (Fig. 2). Expressed relative to respective maximal vasodilatations with SNP, peak ROV tended to increase with branch order (FA<1A<2A<3A). Within each branch,

ROV increased with contraction duration, such that 100<250<500<1000 ms. While the effects of branch order and contraction duration were similar between age groups, respective ROV responses in old mice were generally depressed relative to those in young mice. We have shown previously that force produced by the GM during contraction is not different between age groups (Bearden *et al.* 2004).

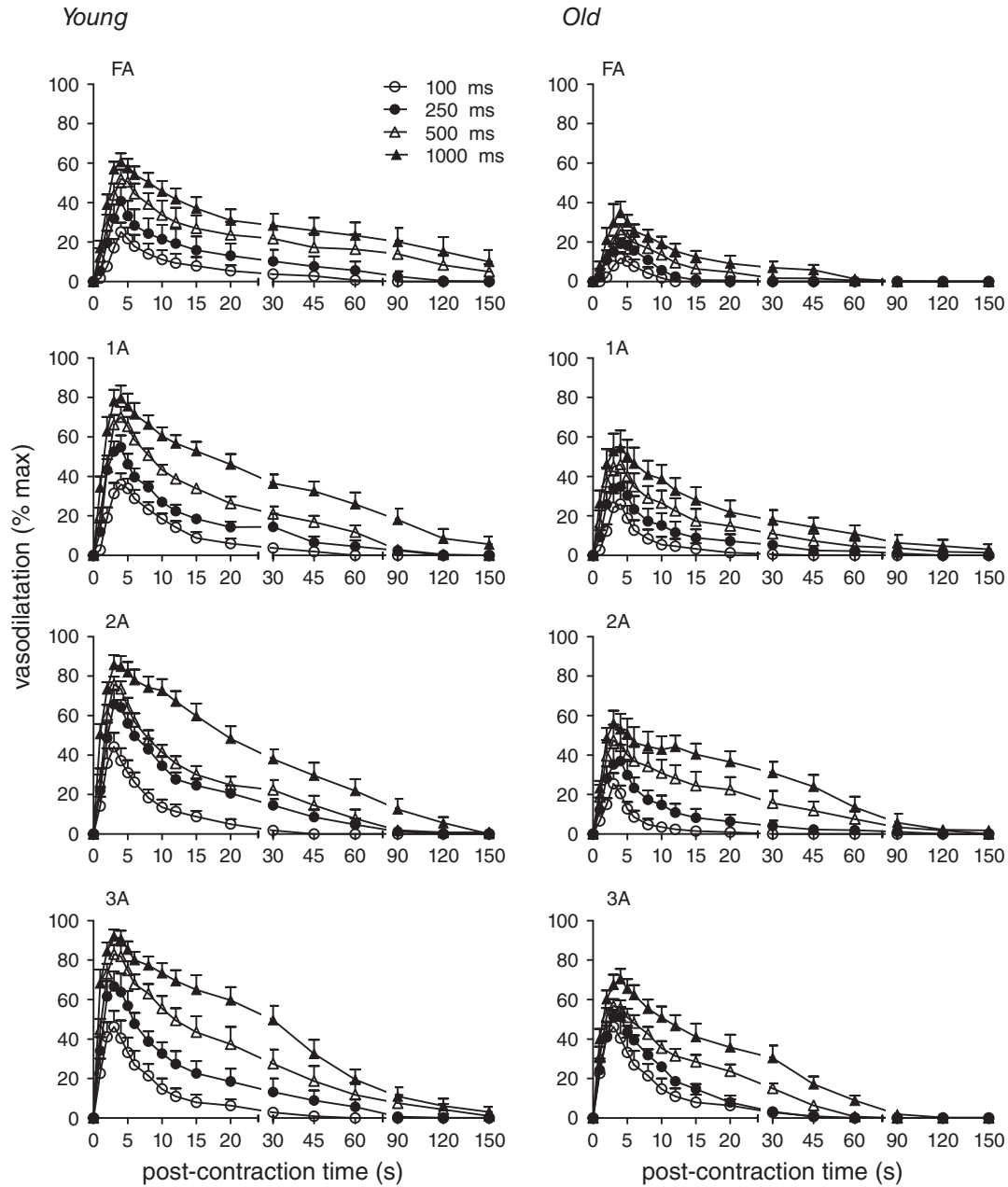


Figure 2. With similar time course, ROV is depressed throughout resistance networks of old versus young mice

For single tetanic contractions of 100, 250, 500, or 1000 ms duration at 100 Hz (key applies to all panels), vasodilatation (expressed in relative terms as % max; see Methods) tended to increase with vessel branch order (FA<1A<2A<3A) and with contraction duration (100<250<500<1000 ms). Across branch orders, ROV was lower for GM in old compared to young mice. Summary data are means \pm SEM, $n = 6$ per age group.

Because of tissue movement and vessel displacement during muscle contraction, it was not possible to precisely determine the time of dilatation onset. Therefore, the initial vasomotor response was evaluated at 1 s following the cessation of contraction after refocusing the vessel image. At this time point, the increase in diameter was greatest in the smaller downstream branches compared to larger upstream branches (FA < 1A < 2A < 3A) (Fig. 3). The initial response also increased with the duration of muscle contraction and these relationships were maintained with responses expressed in either absolute or relative terms (Fig. 3, left and right panels, respectively). Despite maintaining graded responses to contraction duration, these initial dilatations were attenuated by ~half in vessels of old mice compared to young mice, with the inhibitory effect of advanced age most apparent in FAs (Fig. 3).

Expressed in absolute values, peak dilatations were greater in arterioles than in FAs and were similar across 1A, 2A and 3A branch orders within each age group (Fig. 4, left panels). However, peak dilatations in old mice were attenuated by ~half compared to those in young mice. Relative to maximal diameters with SNP, peak dilatations during ROV increased with vessel branch order (FA < 1A < 2A < 3A) and with contraction duration while also attenuated in old mice compared to young mice (Fig. 4, right panels). These differences in ROV between age groups were manifest despite similar resting and maximal diameters between age groups (Fig. 1). The depression of peak ROV with advanced age was greatest in FAs (Fig. 4). In 3As of young mice, peak vasodilatation to 1000 ms contraction approximated maximal diameter with SNP.

Temporal dynamics of ROV are unaffected by ageing

Peak ROV was attained within ~4 s across branch orders (Fig. 5). Within respective branch orders, the time-to-peak for ROV was remarkably consistent across contraction durations. The time-to-peak ROV was longer in FA (~4 s) and 1A (~3.5 s) compared to 2A and 3A (~3 s) branches and this temporal delay for proximal *versus* distal vessels was manifest across durations of muscle contraction. Respective time-to-peak values for ROV were not significantly different between age groups (Fig. 5).

Sympathetic innervation

Perivascular sympathetic innervation was tested by labelling FA with a non-specific neural marker (PGP9.5) and with a selective marker of sympathetic nerves (TH). Respective markers overlapped with each other, indicating the absence of other sources of innervation (Fig. 6). It was not possible to obtain definitive staining of arterioles embedded within the GM due to lack of antibody access in whole-mount preparations and the inability to

isolate intact arteriolar segments from within the muscle. Nevertheless, perivascular sympathetic nerves are known to course along arteriolar networks supplying striated muscle (Marshall, 1982; Boegehold & Johnson, 1988; Hungerford *et al.* 2000).

Differential modulation of ROV by α ARs in young *versus* old mice

To investigate the role of subthreshold α AR stimulation, 10^{-9} M NA was added to the superfusion solution. Alternatively, to investigate the role of constitutively activated α ARs, 10^{-6} M phentolamine was added (Jackson *et al.* 2010). Neither treatment affected resting diameter in either age group (Table 1). Further, neither treatment affected the onset of ROV in either age group (i.e. values at 1 s post contraction were not different from those shown in Fig. 3). Nevertheless, peak ROV was affected differentially in the GM of young *versus* old mice, respectively:

Activation of α ARs attenuates peak ROV in young mice.

Across vessel branch orders and contraction durations, NA attenuated peak ROV in resistance networks of young mice (Fig. 7, left panels), particularly in FA and 1A branches. In contrast, NA had little effect on peak ROV in respective vessel branch orders of old mice (Fig. 7, right panels), where responses were attenuated (compared to young mice) under control conditions.

Inhibition of α ARs improves peak ROV in old mice.

Across vessel branch orders and contraction durations, phentolamine enhanced peak ROV in old mice (Fig. 7, right panels) while having negligible effect in young mice (Fig. 7, left panels).

Complementary experiments confirmed that force produced by the GM during tetanic contractions was unaffected by either NA or phentolamine and that values for old mice were consistent with those for young mice (Fig. 8).

Roles for α AR receptor subtypes

The functional distribution of α_1 ARs and α_2 ARs varies with branch order in arteriolar networks of the GM (Moore *et al.* 2010b). With NA (i.e. α AR stimulation) having the greatest effect in young mice and phentolamine (i.e. α AR inhibition) having the greatest effect in old mice, we used a differential approach to investigate the role of each α AR subtype in respective age groups:

Selective stimulation of α_1 ARs or α_2 ARs attenuates ROV of young mice.

In the GM of young mice, selective stimulation of α_1 ARs with 10^{-7} M PE or of α_2 ARs with 10^{-7} M UK (i.e. using concentrations slightly

above respective thresholds for vasoconstriction; Sinkler & Segal, 2014) attenuated peak ROV across contraction durations, particularly in proximal FA and 1A branches (Fig. 9). Nevertheless, this effect of α AR stimulation diminished as contraction duration increased, particularly in 2A branches. For 3A branches, peak ROV 'escaped' attenuation during activation of either α AR subtype. Thus,

activation of either α_1 ARs or α_2 ARs can blunt peak ROV in proximal branches of resistance networks controlling blood flow to the GM of young mice.

Selective inhibition of α_1 ARs or α_2 ARs enhances ROV of old mice. In the GM of old mice, selective inhibition of α_1 ARs with 10^{-8} M PZ or of α_2 ARs with 10^{-7} M RW

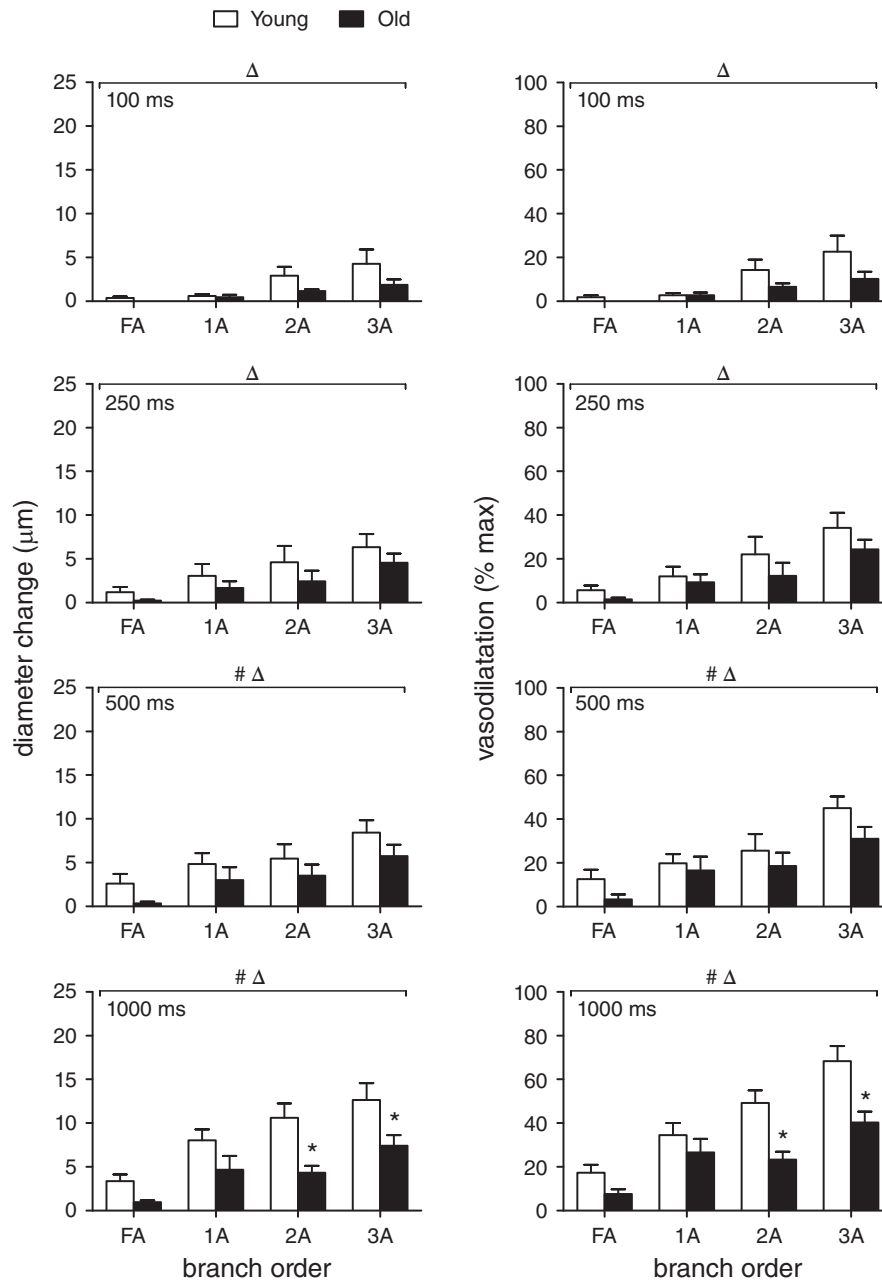


Figure 3. Initiation of ROV increases with contraction duration and branch order but is diminished with advanced age

At 1 s post-contraction, vasodilatation increased with branch order (FA<1A<2A<3A), and contraction duration (all at 100 Hz) whether expressed as absolute diameter change (μ m, left panels) or relative responses (% max, right panels). These initial responses were attenuated for all branch orders in GM of old mice compared to young mice. $\Delta P < 0.05$, main effect of branch order; $\# P < 0.05$, main effect of age. $* P < 0.05$, old vs. young mice within respective branch order. Summary data are means \pm SEM, $n = 6$ per age group.

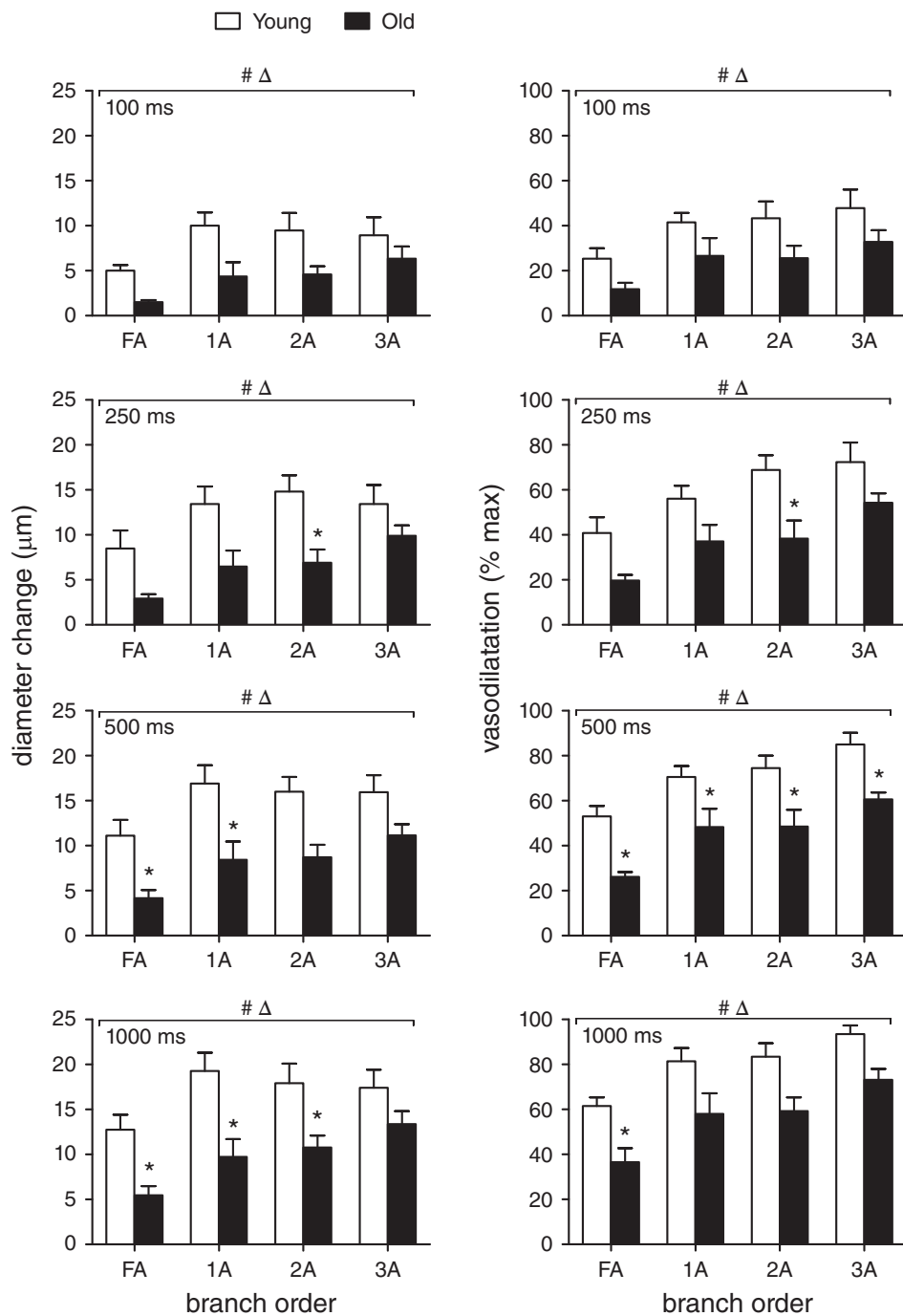


Figure 4. Peak ROV increases with contraction duration and branch order but is diminished with advanced age

Following each contraction duration at 100 Hz, peak vasodilatation expressed as diameter change (μm , left panels) was similar across branch orders while relative responses (% max, right panels) increased with branch order (FA<1A<2A<3A). Both absolute and relative peak ROV increased with contraction duration for all branch orders in both age groups, but peak ROV was diminished consistently in all branch orders for old mice compared to young mice, with the greatest effect of ageing in FA. $\Delta P < 0.05$, main effect of branch order; $\# P < 0.05$, main effect of age, $* P < 0.05$, old vs. young within respective branch order. Summary data are means \pm SEM, $n = 6$ per age group.

increased peak ROV of FAs across contraction durations (Fig. 10). Downstream, α_2 AR inhibition increased peak ROV in 1A but not in 2A or 3A branches, while α_1 AR inhibition had no effect on peak ROV in any arteriolar branch order. These findings illustrate that constitutive activation of respective α AR subtypes exerts the greatest inhibitory effect on peak ROV in FAs, with the effect of α_2 ARs extending into 1A branches. In contrast, peak ROV in 2A and 3A branches was unaffected by selective inhibition of either α AR subtype.

Discussion

Dilations of the resistance vasculature to single brief muscle contractions illustrate the regulatory events at exercise onset that facilitate transitioning from rest to

physical activity; i.e. the rapidity with which blood flow and oxygen delivery can be increased to active skeletal muscle fibres and promote the generation of ATP through oxidative phosphorylation. Advanced age is known to restrict muscle blood flow, in part through the activation of α ARs. This study has defined the kinetics and magnitude of ROV along microvascular resistance networks controlling blood flow to the mouse GM. Further, we have resolved differential modulation of ROV through α ARs in young versus old male mice. In response to single tetanic contractions, ROV typically began within 1 s of muscle contraction and reached peak dilatation within 4 s post contraction and throughout the networks of both young and old mice. The relative magnitude of ROV increased from proximal to distal branches (FA < 1A < 2A < 3A) and increased with contraction duration (100–1000 ms) in

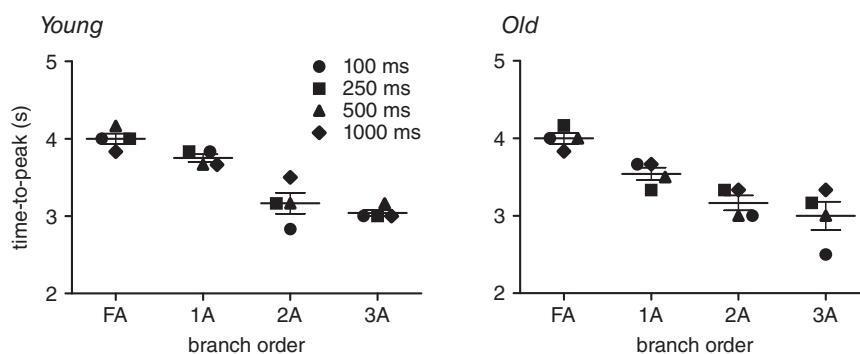


Figure 5. ROV peaks earlier in downstream branches of the resistance network

The time-to-peak for ROV decreased as branch order increased (FA > 1A > 2A > 3A) in GM of both young mice ($R^2 = 0.950$) and old mice ($R^2 = 0.986$). For each branch order, the time-to-peak ROV was consistent across contraction durations for both age groups. Note temporal lag between downstream 3A and upstream FA, particularly in old mice for 100 ms contraction. Each data point represents the mean value for given duration from $n = 6$; horizontal bar for each branch indicates mean time-to-peak \pm SEM across contraction durations.

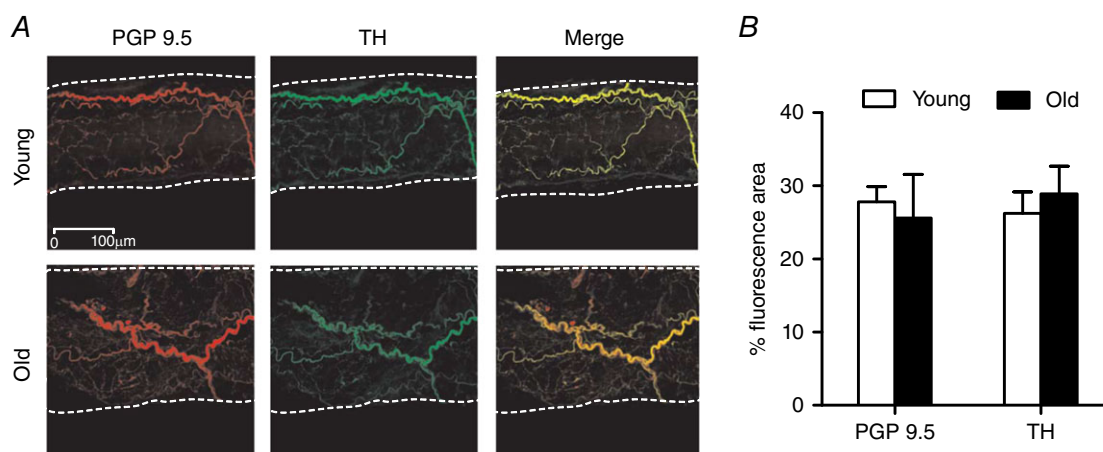


Figure 6. Sympathetic innervation of GM feed arteries for young and old mice

A, representative immunofluorescent staining (maximum Z-stack projection of confocal image slices) of all perivascular nerves (protein gene product 9.5, PGP9.5) and of sympathetic nerves (tyrosine hydroxylase, TH) in GM feed arteries of young and old mice. Vessel edges indicated by dotted lines. B, innervation per vessel surface area (% fluorescence area; see Methods) for PGP9.5 and TH was not different between FAs of young and old mice. Summary data are means \pm SEM, $n = 4$ per age group.

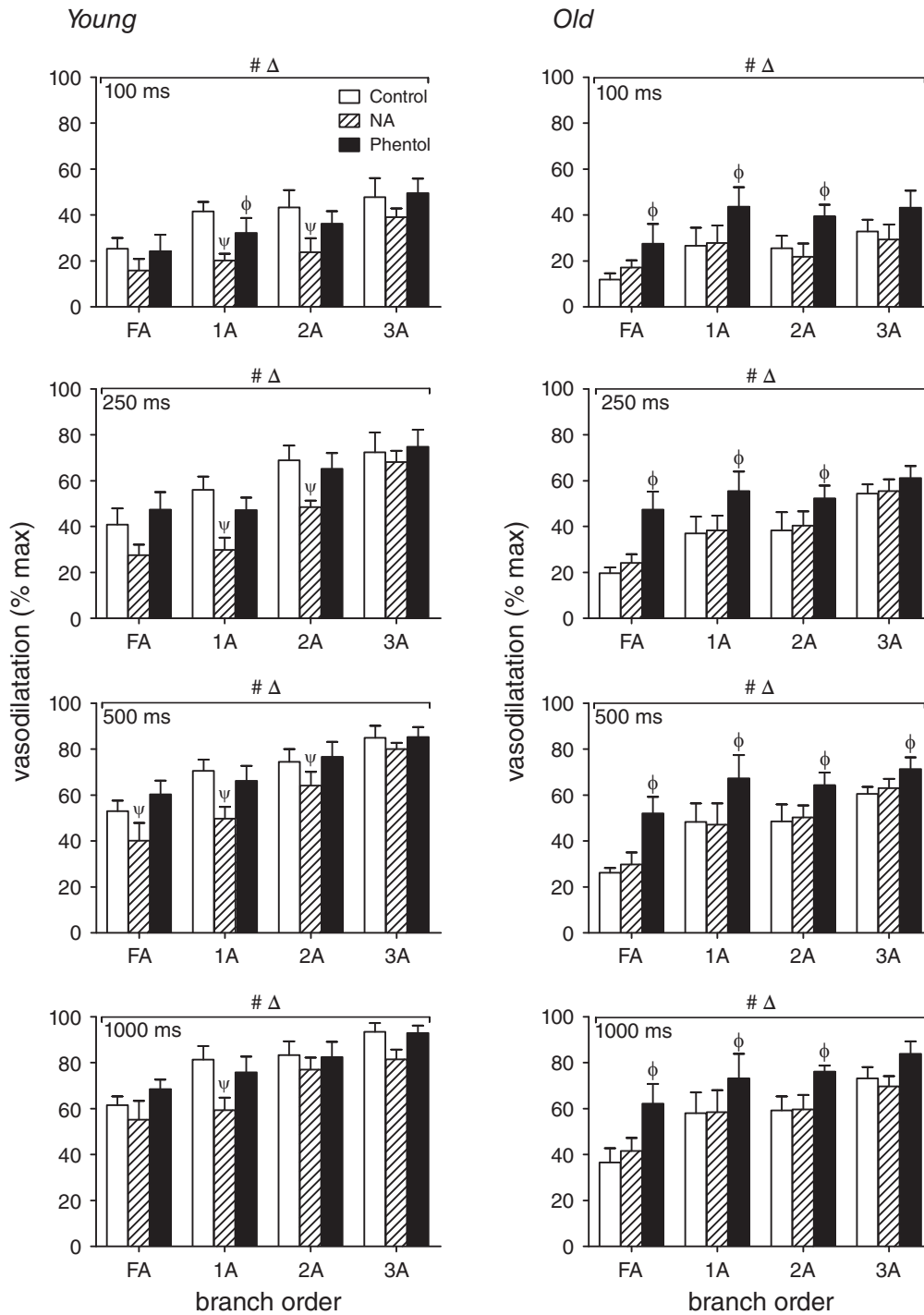


Figure 7. Differential modulation of ROV in GM branch orders by α ARs in young versus old mice
 Peak ROV (% max) in FA, 1A, 2A and 3A following 100, 250, 500 and 1000 ms contraction at 100 Hz in the GM of young and old mice. Peak ROV increased as contraction duration increased in both age groups. Stimulation of α ARs with NA (10^{-9} M) attenuated peak ROV in young mice but not in old mice. In contrast, inhibition of α ARs with phentolamine (Phentol, 10^{-6} M) enhanced peak ROV in old mice but not in young mice. The effect of α AR modulation on peak ROV tended to be greater in FA and 1A than in 2A and 3A. $\Delta P < 0.05$, main effect of branch order. # $P < 0.05$, main effect of Phentol or NA. $\psi P < 0.05$, NA vs. control in designated branch order. $\phi P < 0.05$, Phentol vs. control in designated branch order. Summary data are means \pm SEM, $n = 6$ per age group.

all branch orders. Nevertheless, ROV was depressed in all vessel branches of old compared to young mice despite similar levels of GM force production between age groups. Whereas subthreshold stimulation of α ARs with NA depressed ROV only in young mice, inhibition of α ARs with phentolamine improved ROV only in old mice – yet neither intervention affected resting diameters or GM force production. Thus, subtle manipulation of α ARs has significant physiological consequences on vasomotor control that vary with age. With pharmacological interventions selective for α_1 ARs versus α_2 ARs, activating either AR subtype attenuated ROV in young mice, while inhibiting α_2 ARs was more effective than inhibiting α_1 ARs in restoring ROV for old mice. Integration of these findings uniquely illustrates differential modulation of ROV by ARs in resistance networks of young versus old skeletal muscle. While manifest throughout network branches, the modulation of ROV through α ARs is most effective in upstream branches (FA, 1A) that govern the volume of blood flowing into arteriolar networks. In contrast, downstream 2A and 3A branches, which control the regional distribution of blood flow to capillaries, are less susceptible to modulation through α ARs, particularly as contraction duration increases.

ROV across branch orders

With peak ROV quantified as the actual change in vessel ID, dilatations increased with contraction duration but were similar in magnitude across arteriolar branch orders for each contraction duration (Fig. 4). For a given change in diameter, the net effect on volumetric blood flow will increase with resting ID. In branching networks, the number of segments increases with branch order

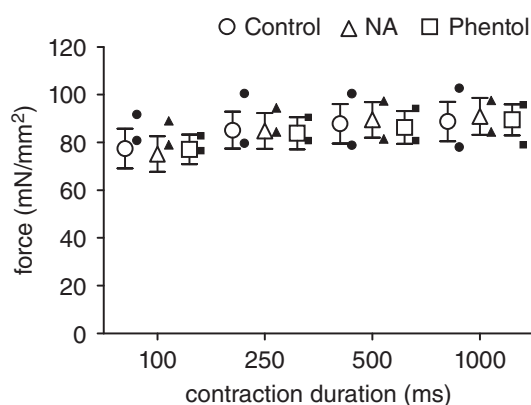


Figure 8. Muscle force production is unaffected during manipulation of adrenoceptor activation

During single tetanic contractions at 100 Hz, active force produced by GM in young ($n = 6$; open symbols, means \pm SEM) and old ($n = 2$, individual solid symbols) mice was similar across contraction durations as well as between control conditions and superfusion with either NA (10^{-9} M) or phentolamine (10^{-6} M).

such that the increase in flow through a parent vessel is distributed among its daughter branches. In contrast, expressing ROV as a percentage of maximal vasodilatation within each branch order (i.e. relative to the dynamic range between resting ID and maximal ID) enables comparison of reactivity across vessels that differ in size and branch order. With such perspective, the present data illustrate the trend for ROV to increase with branch order ($FA < 1A < 2A < 3A$) for each contraction duration and with the duration of contraction across branch orders. Thus, 2A and 3A approach maximal ID in response to our longest contraction duration (Fig. 2). Consistent with findings in hamsters (VanTeeffelen & Segal, 2006) and rats (Novielli & Jackson, 2014), these findings confirm that ROV is more robust in distal compared to proximal branches of the resistance network, in accord with classic studies of vasodilatation (Folkow *et al.* 1971; Granger *et al.* 1976). Nevertheless, ROV was attenuated throughout networks of old mice compared to those of young mice (Figs. 2 and 4). While consistent with an earlier study focused on distributing (2A) arterioles (Jackson *et al.* 2010), the present data demonstrate that the effect of advanced age encompasses the entire resistance network yet does so in a graded manner. Thus, FA dilatations are consistently less than observed in arterioles, underscoring the importance of maintaining resistance to blood flow external to the muscle even as downstream arterioles approach maximum dilatation. As functional sympatholysis is most effective in distal branches (Folkow *et al.* 1971; VanTeeffelen & Segal, 2000), restricting muscle blood flow by inhibiting ascending vasodilatation through α AR activation (Haug *et al.* 2003) effectively maintains peripheral resistance and arterial perfusion pressure when intramuscular arterioles dilate. This role for α AR activation becomes especially important when the energy requirements of aerobic activity become limited by cardiac output (Rowell, 1974).

Initiation of ROV in downstream microvessels ascends into proximal feed arteries

Recording the ID of individual branches at 30 fps throughout each response to GM contraction enabled temporal resolution of vasomotor responses with high fidelity (Fig. 2). With tissue displacement during contraction and time required to refocus, 1 s post contraction was the first time point in which ID was resolved effectively across all durations (Fig. 3). These data illustrate that the initiation of ROV occurs sooner in the distal (i.e. 3A and 2A) branches. Indeed, only the latter microvessels began dilating at 1 s post contraction in response to the shortest (100 ms) contraction. As contraction duration increased, proximal branches were ‘recruited’ in this initial response, albeit to a lesser extent compared to downstream branches. Nevertheless, with negligible differences in ID or vasomotor tone (Fig. 1),

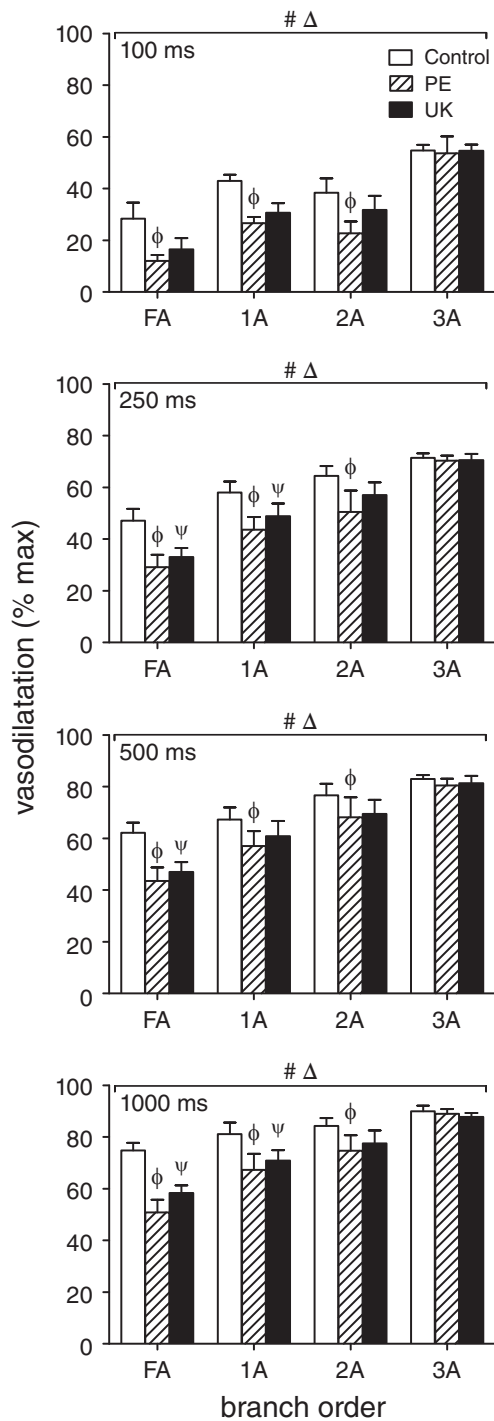


Figure 9. Selective stimulation of α_1 ARs or α_2 ARs attenuates ROV in upstream branches of GM in young mice

Peak ROV (% max) in FA, 1A, 2A and 3A following 100, 250, 500 and 1000 ms contraction in the GM of young mice. Across contraction durations, selective activation of α_1 ARs (PE, 10^{-7} M) or of α_2 ARs (UK, 10^{-7} M) attenuated ROV (% max) in FA, 1A and 2A but had no effect on ROV in 3A. $\Delta P < 0.05$ main effect of branch order; $\#P < 0.05$ main effect of treatment; $\Phi P < 0.05$, PE vs. control, $\Psi P < 0.05$, UK vs. control. Summary data are means \pm SEM for $n = 6$ young mice.

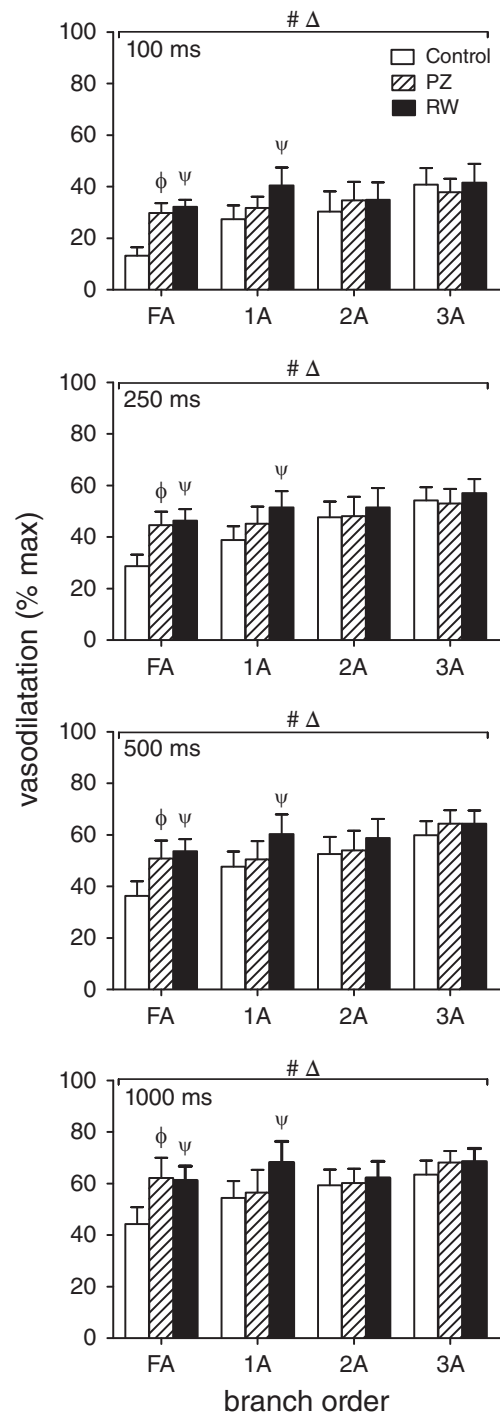


Figure 10. Selective inhibition of α_1 ARs or α_2 ARs improves ROV in upstream branch orders of GM in old mice

Peak ROV (% max) in FA, 1A, 2A and 3A following 100, 250, 500 and 1000 ms contraction in the GM of old mice. Across contraction durations, selective inhibition of α_1 ARs (PZ, 10^{-8} M) or of α_2 ARs (RW, 10^{-7} M) improved ROV in FA while inhibition of α_2 ARs improved ROV in 1A. Nevertheless, inhibition of either α AR subtype alone had no effect in 2A or 3A. $\Delta P < 0.05$ main effect of branch order; $\#P < 0.05$, main effect of treatment; $\Phi P < 0.05$, PZ vs. control, $\Psi P < 0.05$, RW vs. control. Summary data are means \pm SEM for $n = 6$ old mice.

respective branches of networks supplying the GM of old mice were consistently less responsive than those of young mice (Fig. 3). Even though this distal-to-proximal evolution of ROV is subtle during peak dilatation (Fig. 4, right panels), the inhibitory effect of advanced age is manifest throughout.

Because FAs are external to the tissue, they are not affected directly by contracting muscle fibres. Thus ROV in FAs reflects ascending vasodilatation initiated within the muscle fibres in response to muscle contraction (Hilton, 1959; Folkow *et al.* 1971; Segal & Jacobs, 2001; VanTeeffelen & Segal, 2006). The ~ 1 s delay between peak ROV in proximal FAs (~ 4 s) compared to peak ROV in distal 3As (~ 3 s) strengthens this interpretation. Further, ROV occurs first in the smallest arterioles located furthest downstream (Figs. 3 and 5), which in turn may reflect signals originating from terminal arterioles and capillaries (Segal, 1991; Song & Tyml, 1993; Berg *et al.* 1997; Beach *et al.* 1998) most intimately associated with skeletal muscle fibres. The dilatation of distal arterioles will promptly increase capillary perfusion while total flow increases as dilatation ascends the resistance network (Segal & Duling, 1986). The rapid onset of vasodilatation and its ability to ascend the arteriolar network into FAs are consistent with conducted vasodilatation mediated by electrical signal transmission along the vessel wall (Segal & Jacobs, 2001). Thus, ROV within each vessel branch order may entail activation of membrane ion channels in microvessels responding to muscle fibre contraction. Indeed, a likely signal for the initiation of ROV is hyperpolarization of the endothelium (Emerson & Segal, 2000), e.g. through activation of K^+ channels (Armstrong *et al.* 2007; Behringer & Segal, 2012; Crecelius *et al.* 2013).

The present data reveal a temporal gradient along the resistance network, with peak ROV occurring progressively later in upstream *versus* downstream branches (Fig. 5). This coordinated behaviour is consistent with earlier reports of vasodilatation originating within arteriolar networks ascending into the proximal arterial supply (Hilton, 1959; Folkow *et al.* 1971; Segal & Jacobs, 2001; VanTeeffelen & Segal, 2006). A key finding here is the consistency of time-to-peak ROV within each branch order across contraction durations (Fig. 5), even while response amplitude increases with contraction duration (Figs. 2 and 4; VanTeeffelen & Segal, 2006; Jackson *et al.* 2010; Novielli & Jackson, 2014). As this spatio-temporal relationship is maintained during advanced age, we suggest that the signal(s) mediating the initiation and time course of ROV are unaffected by ageing even while the response amplitude (i.e. peak ROV) is attenuated.

When the kinetics of ROV in the mouse GM (Fig. 2) are compared to ROV kinetics recorded in human subjects performing single contractions of the forearm (Carlson *et al.* 2008; Casey & Joyner, 2012; Crecelius *et al.* 2013) or knee extensors (Credeur *et al.* 2015), respective

time courses are remarkably similar, peaking ~ 4 – 5 s post contraction across respective ranges of contraction intensities. While the temporal correspondence of these integrated responses is apparent, the distal-to-proximal gradient in time-to-peak ROV along the resistance network is resolved here for the first time. If such a temporal gradient occurs along resistance networks in humans, it is masked when evaluating ROV via blood flow responses in the principal artery (e.g. brachial or femoral) supplying musculature in the active limb. Nevertheless, the overall correspondence of ROV kinetics between mice and humans lends further support to the mouse as a viable model to gain mechanistic insight into how advanced age (or experimental intervention) affects ROV. As illustrated here, a key feature and unique advantage of directly observing the intact microcirculation is the ability to determine what happens where and when along resistance networks that control blood flow to skeletal muscle.

Attenuated ROV with advanced age

Refining our surgical approach enabled exposure of the inferior gluteal artery (the FA studied here) along with arteriolar networks embedded within the GM. At the earliest time point resolved (1 s post contraction), vasodilatation was blunted throughout networks of old mice compared to young mice and this effect of advanced age was most pronounced in FAs (Fig. 3). These data illustrate that advanced age delays the initiation of ROV, particularly in proximal branches with brief contractions. Thus, the coupling between contractile activity and the rapid onset of vasodilatation loses sensitivity with ageing, which points to a defect in the underlying signalling events. Supporting this conclusion are the reductions in peak ROV for all branch orders at each contraction duration in old compared to young mice (Figs. 2 and 4). Recent findings show that activation of small- and intermediate-conductance Ca^{2+} activated K^+ channels in the endothelium of FAs from old mice dissipated electrical signals more effectively when compared to the endothelium of FAs from young mice, attributable to charge dissipation through 'leaky' membranes (Behringer *et al.* 2013). In light of the present data, such an effect on electrical signalling would blunt the initiation of hyperpolarization and restrict conducted vasodilatation (as shown in the GM; Bearden *et al.* 2004) as well as ascending dilatation (Fig. 3). Further studies are required to resolve the role of the endothelium and of specific K^+ channels in the initiation of ROV and ascending vasodilatation.

Non-selective manipulation of α ARs. In the GM of young mice, stimulation with NA attenuated peak ROV across all branch orders and did so at a concentration (10^{-9} M) that had no effect on resting diameters (Table 1). This effect of subthreshold α AR stimulation was greatest in

proximal FA and 1A branches while nearly absent in distal 3A branches (Fig. 7, left panels). Such behaviour is consistent with the ability of distal branches to more readily escape from sympathetic vasoconstriction during muscle contraction when compared to proximal arterioles or FAs (Folkow *et al.* 1971; VanTeeffelen & Segal, 2000), probably due to their being more intimately associated with active muscle fibres and vasodilator metabolites. In contrast, 10^{-9} M NA had no effect on ROV of vessels in the GM of old mice under control conditions, suggesting that the attenuation of ROV (compared to young mice) was due to a preexisting level of α AR activation not less than obtained with 10^{-9} M NA. In contrast, an earlier study found that 10^{-9} M NA attenuated ROV in 2A of male mice at 20 months of age (Jackson *et al.* 2010). Whereas 20 months in the mouse corresponds to humans in their early 60s, mice at 24 months of age correspond to late 60s in humans (Flurkey *et al.* 2007), where constitutive activation of α ARs may be greater. Nevertheless, and consistent with earlier findings, non-selective inhibition of α ARs with phentolamine improved peak ROV in old (but not young) mice (Fig. 7).

Previous studies have implicated a role for α AR stimulation in the attenuation of ROV with advanced age (Jackson *et al.* 2010; Casey & Joyner, 2012). The present data uniquely illustrate that ROV is inhibited to the greatest extent in proximal branches. Restoration of ROV during α AR inhibition was greatest in FAs, which are positioned to control the total volume of blood flowing into the tissue. That FAs are a key site for restricting ROV during advanced age is consistent with blood flow in 2A branches remaining significantly lower in old compared to young mice despite no difference in respective diameters or dilatations during rhythmic contractions of the GM (Jackson *et al.* 2010). The activation of α ARs inhibits conducted (and ascending) vasodilatation of FAs (Haug *et al.* 2003; VanTeeffelen & Segal, 2003) and may well explain the attenuation of conducted vasodilatation along arterioles in old mice (Bearden *et al.* 2004). This conclusion is supported by the restriction of ROV to the active (inferior) region of the GM until α ARs were inhibited by phentolamine; vasodilation then spread to the inactive (superior) region of the muscle (Moore *et al.* 2010a). In turn we suggest that constitutively enhanced SNA (Dinenno *et al.* 1999) and α AR stimulation (Jackson *et al.* 2010; Casey & Joyner, 2012) during advanced age effectively restrict muscle blood flow by attenuating the dilatation of FAs.

Roles of α_1 ARs and α_2 ARs. In light of the non-uniform distribution of α AR subtypes along arteriolar networks of the mouse GM (Moore *et al.* 2010b), finding that α AR stimulation attenuated ROV in young mice while α AR inhibition restored ROV in old mice led us to resolve the role of α AR subtypes for respective age groups. Agents

selective for stimulating α_1 ARs (PE) versus α_2 ARs (UK) were tested in young mice while agents selective for inhibiting α_1 ARs (PZ) versus α_2 ARs (RW) were tested in old mice in accord with their efficacy and selectivity (Moore *et al.* 2010b; Sinkler & Segal, 2014). To ensure that PE and UK were exerting effects, each was applied at a concentration (10^{-7} M) just above the threshold for eliciting vasoconstriction (Sinkler & Segal, 2014). In young mice, stimulating either α_1 ARs with PE or α_2 ARs with UK attenuated ROV similarly. Across contraction durations, this effect was greatest in FAs and decreased as branch order increased, with negligible effect in 3A (Fig. 9). In old mice, the inhibition of either α_1 ARs or α_2 ARs had complementary effects on restoring ROV in FAs. However, in 1A branches only the inhibition of α_2 ARs improved ROV, consistent with vasoconstriction to NA (i.e. the non-selective physiological agonist for ARs) being dominated by α_2 ARs in this branch order of the GM (Moore *et al.* 2010b). Unlike the ability of non-selective inhibition of both α AR subtypes (with phentolamine) to improve ROV in nearly all branch orders in old mice (Fig. 7, right panels), neither of the selective α AR antagonists applied alone improved ROV in 2A or 3A branches (Fig. 10). Thus, activation of either α AR subtype can attenuate ROV in downstream arterioles.

Summary and perspective

By locally stimulating the GM in anaesthetized mice, the present study avoided potentially confounding effects of central command on cardiovascular regulation (Ishii *et al.* 2012). Further, our pharmacological manipulations of α AR stimulation and inhibition were constrained to the GM by the addition of respective agents to the superfusion solution, thereby avoiding systemic effects and the possibility of evoking cardiovascular reflexes. Complementary experiments verified that manipulating α AR activation was without effect on the force produced during GM contraction. In such manner, our experimental paradigms emulate local infusion of α AR agonists and antagonists into the human forearm during contractions involving a relatively small muscle mass (Dinenno *et al.* 2002; Casey & Joyner, 2012). Our findings illustrate that, despite no effect on resting diameters or vasomotor tone, constitutive activation of α ARs during advanced age depressed ROV in all branch orders of resistance networks controlling skeletal muscle blood flow. This effect of ageing was reversed by inhibiting α ARs with phentolamine and was recapitulated in young mice by stimulating α ARs with NA at a concentration (10^{-9} M) that had no effect on vessel diameters. Our data thereby illustrate a subtle yet physiologically significant role for α ARs in modulating ROV.

Whilst consistent with reports of attenuated ROV during advanced age in human subjects (Carlson *et al.* 2008; Casey & Joyner, 2012), this is the first study to

identify where α AR subtypes predominate in modulating ROV among branches of the resistance vasculature and to demonstrate differential modulation of ROV according to age. In old mice, attenuation of ROV was greater in FA and 1A branches compared to 2A and 3A branches. Further, selective inhibition of α_2 ARs (rauwolscine; 10^{-7} M) restored ROV more effectively than did inhibiting α_1 ARs (prazosin; 10^{-8} M), indicating that the attenuation of ROV with advanced age is most effective in proximal branches via constitutive activation of α_2 ARs. In young mice, non-selective stimulation of α ARs with NA depressed ROV most effectively in FA and 1A branches while 2A and 3A branches escaped such an effect. In turn, selective stimulation of α_1 ARs with phenylephrine (10^{-7} M) or of α_2 ARs with UK 14304 (10^{-7} M) attenuated ROV primarily in FAs. Prior studies in humans have implied that functional sympatholysis is impaired during advanced age (Dinenno *et al.* 2005; Kirby *et al.* 2011). Consistent with this interpretation, the present findings illustrate that ROV is attenuated throughout the resistance network in old mice compared to young mice and does so in a manner that is greatest in FAs. Attenuation of ROV in these proximal branches during advanced age will restrict the volume of blood entering the muscle. In distal branches, the attenuation of ROV can adversely affect blood flow distribution to active muscle fibres. These concerted effects help to explain the impairment in functional sympatholysis that is manifest during advancing age, which thereby contributes to the difficulty in transitioning from rest to muscular activity or to an increase from moderate to more intense levels of physical exertion.

References

- Armstrong ML, Dua AK & Murrant CL (2007). Potassium initiates vasodilatation induced by a single skeletal muscle contraction in hamster cremaster muscle. *J Physiol* **581**, 841–852.
- Beach JM, McGahren ED & Duling BR (1998). Capillaries and arterioles are electrically coupled in hamster cheek pouch. *Am J Physiol Heart Circ Physiol* **275**, H1489–H1496.
- Bearden SE, Payne GW, Chisty A & Segal SS (2004). Arteriolar network architecture and vasomotor function with ageing in mouse gluteus maximus muscle. *J Physiol* **561**, 535–545.
- Behringer EJ & Segal SS (2012). Spreading the signal for vasodilatation: implications for skeletal muscle blood flow control and the effects of ageing. *J Physiol* **590**, 6277–6284.
- Behringer EJ, Shaw RL, Westcott EB, Socha MJ & Segal SS (2013). Aging impairs electrical conduction along endothelium of resistance arteries through enhanced Ca^{2+} -activated K^+ channel activation. *Arterioscler Thromb Vasc Biol* **33**, 1892–1901.
- Berg BR, Cohen KD & Sarelius IH (1997). Direct coupling between blood flow and metabolism at the capillary level in striated muscle. *Am J Physiol Heart Circ Physiol* **272**, H2693–H2700.
- Boegehold MA & Johnson PC (1988). Response of arteriolar network of skeletal muscle to sympathetic nerve stimulation. *Am J Physiol Heart Circ Physiol* **254**, H919–H928.
- Boerman EM & Segal SS (2016). Depressed perivascular sensory innervation of mouse mesenteric arteries with advanced age. *J Physiol* **594**, 2323–2338.
- Carlson RE, Kirby BS, Voyles WF & Dinenno FA (2008). Evidence for impaired skeletal muscle contraction-induced rapid vasodilation in aging humans. *Am J Physiol Heart Circ Physiol* **294**, H1963–H1970.
- Casey DP & Joyner MJ (2012). Influence of α -adrenergic vasoconstriction on the blunted skeletal muscle contraction-induced rapid vasodilation with aging. *J Appl Physiol* **113**, 1201–1212.
- Corcondilas A, Koroxenidis GT & Shepherd JT (1964). Effect of a brief contraction of forearm muscles on forearm blood flow. *J Appl Physiol* **19**, 142–146.
- Crecelesius AR, Kirby BS, Luckasen GJ, Larson DG & Dinenno FA (2013). Mechanisms of rapid vasodilation after a brief contraction in human skeletal muscle. *Am J Physiol Heart Circ Physiol* **305**, H29–H40.
- Credeur DP, Holwerda SW, Restaino RM, King PM, Crutcher KL, Laughlin MH, Padilla J & Fadel PJ (2015). Characterizing rapid-onset vasodilation to single muscle contractions in the human leg. *J Appl Physiol* **118**, 455–464.
- Dinenno FA, Dietz NM & Joyner MJ (2002). Aging and forearm postjunctional α -adrenergic vasoconstriction in healthy men. *Circulation* **106**, 1349–1354.
- Dinenno FA, Jones PP, Seals DR & Tanaka H (1999). Limb blood flow and vascular conductance are reduced with age in healthy humans: relation to elevations in sympathetic nerve activity and declines in oxygen demand. *Circulation* **100**, 164–170.
- Dinenno FA, Masuki S & Joyner MJ (2005). Impaired modulation of sympathetic α -adrenergic vasoconstriction in contracting forearm muscle of ageing men. *J Physiol* **567**, 311–321.
- Dodd LR & Johnson PC (1993). Antagonism of vasoconstriction by muscle contraction differs with α -adrenergic subtype. *Am J Physiol Heart Circ Physiol* **264**, H892–H900.
- Emerson GG & Segal SS (2000). Endothelial cell pathway for conduction of hyperpolarization and vasodilation along hamster feed artery. *Circ Res* **86**, 94–100.
- Faber JE (1988). In situ analysis of α -adrenoceptors on arteriolar and venular smooth muscle in rat skeletal muscle microcirculation. *Circ Res* **62**, 37–50.
- Fernando CA, Liu Y, Sowa G & Segal SS (2016). Attenuated rapid-onset vasodilation with greater force production in skeletal muscle of caveolin-2^{-/-} mice. *Am J Physiol Heart Circ Physiol* **311**, H415–H425.
- Fisher JP & Paton JF (2012). The sympathetic nervous system and blood pressure in humans: implications for hypertension. *J Hum Hypertens* **26**, 463–475.
- Flurkey K, Curren J & Harrison D (2007). The mouse in aging research. In *The Mouse in Biomedical Research*, eds Fox JG, Davisson MT, Quimby FW, Barthold SW, Newcomer CE & Smith AL, pp. 637–672. American College of Laboratory Animal Medicine (Elsevier), Burlington.

- Folkow B, Sonnenschein RR & Wright DL (1971). Loci of neurogenic and metabolic effects on precapillary vessels of skeletal muscle. *Acta Physiol Scand* **81**, 459–471.
- Granger HJ, Goodman AH & Granger DN (1976). Role of resistance and exchange vessels in local microvascular control of skeletal muscle oxygenation in the dog. *Circ Res* **38**, 379–385.
- Haug SJ, Welsh DG & Segal SS (2003). Sympathetic nerves inhibit conducted vasodilatation along feed arteries during passive stretch of hamster skeletal muscle. *J Physiol* **552**, 273–282.
- Hilton SM (1959). A peripheral arterial conducting mechanism underlying dilatation of the femoral artery and concerned in functional vasodilatation in skeletal muscle. *J Physiol* **149**, 93–111.
- Hungerford JE, Sessa WC & Segal SS (2000). Vasomotor control in arterioles of the mouse cremaster muscle. *FASEB J* **14**, 197–207.
- Ishii K, Liang N, Oue A, Hirasawa A, Sato K, Sadamoto T & Matsukawa K (2012). Central command contributes to increased blood flow in the noncontracting muscle at the start of one-legged dynamic exercise in humans. *J Appl Physiol* **112**, 1961–1974.
- Jackson DN, Moore AW & Segal SS (2010). Blunting of rapid onset vasodilatation and blood flow restriction in arterioles of exercising skeletal muscle with ageing in male mice. *J Physiol* **588**, 2269–2282.
- Kirby BS, Crecelius AR, Voyles WF & Dinunno FA (2011). Modulation of postjunctional α -adrenergic vasoconstriction during exercise and exogenous ATP infusions in ageing humans. *J Physiol* **589**, 2641–2653.
- Lampa SJ, Potluri S, Norton AS & Laskowski MB (2004). A morphological technique for exploring neuromuscular topography expressed in the mouse gluteus maximus muscle. *J Neurosci Methods* **138**, 51–56.
- Lexell J (1995). Human aging, muscle mass, and fiber type composition. *J Gerontol A Biol Sci Med Sci* **50A** (Special Issue), 11–16.
- Looft-Wilson RC, Haug SJ, Neuffer PD & Segal SS (2004). Independence of connexin expression and vasomotor conduction from sympathetic innervation in hamster feed arteries. *Microcirculation* **11**, 397–408.
- McCarty R, Pacak K, Goldstein DS & Eisenhofer G (1997). Regulation of peripheral catecholamine responses to acute stress in young adult and aged F-344 rats. *Stress* **2**, 113–122.
- Manttari S & Jarvilehto M (2005). Comparative analysis of mouse skeletal muscle fibre type composition and contractile responses to calcium channel blocker. *BMC Physiol* **5**, 4.
- Marshall JM (1982). The influence of the sympathetic nervous system on individual vessels of the microcirculation of skeletal muscle of the rat. *J Physiol* **332**, 169–186.
- Mihok ML & Murrant CL (2004). Rapid biphasic arteriolar dilations induced by skeletal muscle contraction are dependent on stimulation characteristics. *Can J Physiol Pharmacol* **82**, 282–287.
- Moore AW, Bearden SE & Segal SS (2010a). Regional activation of rapid onset vasodilatation in mouse skeletal muscle: regulation through α -adrenoreceptors. *J Physiol* **588**, 3321–3331.
- Moore AW, Jackson WF & Segal SS (2010b). Regional heterogeneity of α -adrenoreceptor subtypes in arteriolar networks of mouse skeletal muscle. *J Physiol* **588**, 4261–4274.
- Novielli NM & Jackson DN (2014). Contraction-evoked vasodilatation and functional hyperaemia are compromised in branching skeletal muscle arterioles of young pre-diabetic mice. *Acta Physiol (Oxf)* **211**, 371–384.
- Reis DJ, Ross RA & Joh TH (1977). Changes in the activity and amounts of enzymes synthesizing catecholamines and acetylcholine in brain, adrenal medulla, and sympathetic ganglia of aged rat and mouse. *Brain Res* **136**, 465–474.
- Remensnyder JP, Mitchell JH & Sarnoff SJ (1962). Functional sympatholysis during muscular activity. Observations on influence of carotid sinus on oxygen uptake. *Circ Res* **11**, 370–380.
- Rowell LB (1974). Human cardiovascular adjustments to exercise and thermal stress. *Physiol Rev* **54**, 75–159.
- Saltin B, Henriksson J, Nygaard E, Andersen P & Jansson E (1977). Fiber types and metabolic potentials of skeletal muscles in sedentary man and endurance runners. *Ann NY Acad Sci* **301**, 3–29.
- Seals DR (1989a). Influence of muscle mass on sympathetic neural activation during isometric exercise. *J Appl Physiol* **67**, 1801–1806.
- Seals DR (1989b). Sympathetic neural discharge and vascular resistance during exercise in humans. *J Appl Physiol* **66**, 2472–2478.
- Segal SS (1991). Microvascular recruitment in hamster striated muscle: role for conducted vasodilatation. *Am J Physiol Heart Circ Physiol* **261**, H181–H189.
- Segal SS (2005). Regulation of blood flow in the microcirculation. *Microcirculation* **12**, 33–45.
- Segal SS & Duling BR (1986). Communication between feed arteries and microvessels in hamster striated muscle: segmental vascular responses are functionally coordinated. *Circ Res* **59**, 283–290.
- Segal SS & Jacobs TL (2001). Role for endothelial cell conduction in ascending vasodilatation and exercise hyperaemia in hamster skeletal muscle. *J Physiol* **536**, 937–946.
- Sinkler SY & Segal SS (2014). Aging alters reactivity of microvascular resistance networks in mouse gluteus maximus muscle. *Am J Physiol Heart Circ Physiol* **307**, H830–H839.
- Song H & Tyml K (1993). Evidence for sensing and integration of biological signals by the capillary network. *Am J Physiol Heart Circ Physiol* **265**, H1235–H1242.
- Thompson RJ, Doran JF, Jackson P, Dhillion AP & Rode J (1983). PGP 9.5 – a new marker for vertebrate neurons and neuroendocrine cells. *Brain Res* **278**, 224–228.
- Tschakovsky ME, Shoemaker JK & Hughson RL (1996). Vasodilation and muscle pump contribution to immediate exercise hyperemia. *Am J Physiol Heart Circ Physiol* **271**, H1697–H1701.
- VanTeeffelen JW & Segal SS (2000). Effect of motor unit recruitment on functional vasodilatation in hamster retractor muscle. *J Physiol* **524**, 267–278.
- VanTeeffelen JW & Segal SS (2003). Interaction between sympathetic nerve activation and muscle fibre contraction in resistance vessels of hamster retractor muscle. *J Physiol* **550**, 563–574.

VanTeeffelen JW & Segal SS (2006). Rapid dilation of arterioles with single contraction of hamster skeletal muscle. *Am J Physiol Heart Circ Physiol* **290**, H119–H127.

Additional information

Competing interests

The authors declare no competing interests. The content of this article is solely the responsibility of the authors and does not necessarily represent the official views of the National Institutes of Health or the American Heart Association.

Author contributions

S.Y.S. and S.S.S. conceived and designed the experiments. S.Y.S. and C.A.F. performed these experiments in the laboratory of S.S.S. All authors analysed and interpreted the data. S.Y.S. prepared the figures and drafted the manuscript. S.S.S. and C.A.F.

edited the manuscript and figures. All authors have approved the final version of the manuscript and agree to be accountable for all aspects of the work. All persons designated as authors qualify for authorship, and all those who qualify for authorship are listed.

Funding

This research was supported by predoctoral fellowship 15PRE22840000 from the Midwest Affiliate of the American Heart Association (to S.Y.S.) and the National Institutes of Health grants R01-HL086483 and R37-HL041026 from the United States Public Health Service (to S.S.S.).

Acknowledgements

Dr Michael J. Davis (University of Missouri) provided the software used for recording and analysing the vasomotor responses in these experiments. Dr Erika M. Boerman (University of Missouri) assisted in the analysis of perivascular innervation density.